Simulation Study of Radial Heat and Mass Transfer inside a Fixed Bed Catalytic Reactor
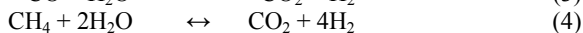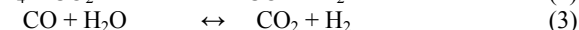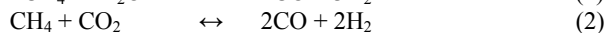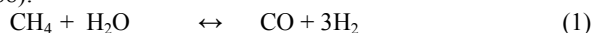
K. Vakhshouri[1], M.M. Y. Motamed Hashemi[2]

Abstract—A rigorous two-dimensional model is developed for simulating the operation of a less-investigated type steam reformer having a considerably lower operating Reynolds number, higher tube diameter, and non-availability of extra steam in the feed compared with conventional steam reformers. Simulation results show that reasonable predictions can only be achieved when certain correlations for wall to fluid heat transfer equations are applied. Due to severe operating conditions, in all cases, strong radial temperature gradients inside the reformer tubes have been found. Furthermore, the results show how a certain catalyst loading profile will affect the operation of the reformer.

Keywords—Steam Reforming, Direct Reduction, Heat Transfer, Two-Dimensional Model, Simulation

I. INTRODUCTION

STEAM reforming is the reaction of a hydrocarbon, especially methane, with the oxidants water vapor and/or carbon dioxide to produce hydrogen and carbon monoxide. The chemical reactions taking place in catalytic methane reforming are numerous, among which four reactions are more probable under the reforming conditions (Hyman, 1968):

$$CH_4 + H_2O \quad \leftrightarrow \quad CO + 3H_2 \qquad (1)$$
$$CH_4 + CO_2 \quad \leftrightarrow \quad 2CO + 2H_2 \qquad (2)$$
$$CO + H_2O \quad \leftrightarrow \quad CO_2 + H_2 \qquad (3)$$
$$CH_4 + 2H_2O \quad \leftrightarrow \quad CO_2 + 4H_2 \qquad (4)$$

A typical reformer generally uses nickel catalysts to accelerate reforming reactions. The reforming reactions are highly endothermic, meaning that large quantities of heat must be added for the reactions to proceed. This is done by reformer fire-box.

Under industrial reforming conditions, carbon deposition can occur as in the Boudourd, Beggs, and methane cracking reactions respectively:

$$2CO \quad \leftrightarrow CO_2 + C \qquad (5)$$
$$CO + H_2 \leftrightarrow C + H_2O \qquad (6)$$
$$2CH_4 \quad \leftrightarrow C + 2H_2 \qquad (7)$$

While conventional steam reformers have been used around the world for over 50 years in such varied industries as refineries, ammonia production, and methanol plants, the production of syngas for reducing iron ores in natural gas based direct reduction (DR) plants, like Midrex® process, has been less investigated. Direct reduction of iron is the first step in converting raw iron ore to steel. The iron ore, which is primarily iron oxide, is contacted with a syngas stream through a moving bed reactor to remove oxygen from the raw iron in the following manner:

$$Fe_2O_3 + 3(H_2/CO) = 2Fe + 3(H_2O/CO_2) \qquad (8)$$
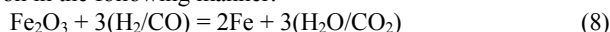
Direct reduced iron (DRI) known as sponge iron can then be treated to produce desired steel products.

II. EXPLANATION OF OPERATIONAL SEVERE CONDITIONS

A Midrex® reformer differs from the conventional steam-reformers in several ways:

• A typical steam-reformer operates at pressures of 20 to 40 bars, but the Midrex® reformer operates at pressures of 2 to 3 bars. Shorter tube length and larger tube diameter in a Midrex® reformer impose less pressure drop compared with the conventional steam-reformers.

• At high mass velocities in conventional steam reformers (G_M = 10 to 23 kg/m²/sec), the radial diffusivity will be too high to allow the development of significant radial concentration. However, in a Midrex® reformer, mass velocities are considerably lower (G_M = 2 to 5 kg/m²/sec), and significant radial gradients may develop inside the tubes. This, in turn, increases residence time and hence, the risk of carbon formation is amplified (Rostrup-Nielsen, 1984).

• In a Midrex® process, design specifications necessitate that the reformer feed gas be a mixture of the off gas stream from the moving bed reactor and fresh natural gas. Since hydrogen and carbon-oxide comprise more than half of the off gas stream, the reformer feed gas is far above the equilibrium condition. As a result, at typical feed temperatures of about 400 °C - 500 °C, set by process economics [11], the reforming reactions can not proceed, whereas the carbon formation reactions have a high potential of stepping up. Moreover, this relatively low temperature of feed gas results in a very large gradient between the furnace gas temperature and process gas temperature at the reactor inlet zone, which consequently develops a large gradient inside the tubes.

• The carbon dioxide content of feed gas in a Midrex® reformer is significantly higher than most conventional steam-reformers. This specification, together with a low content of steam, dictated by design specifications, entails a greater risk of carbon deposits, which must be balanced by selecting appropriate operating reaction parameters and catalysts.

III. STEAM REFORMING MODELING

Published reports about the application of two-dimensional models for simulating industrial steam-reformers are few in number. Reference [25] applied a pseudo-homogeneous two-dimensional model for a steam reformer for

[1] K. Vakhshouri is with Chemical and Biological Engineering Department, University of British Columbia, Vancouver, Canada, V6T 1Z3, Phone: 604-827-5197 e-mail: kvakhshouri@chml.ubc.ca

[2] M.M.Y.M. Hashemi is with Mork Family Department of Chemical Engineering and Material Sciences, University of Southern California, California, USA

the first time. It emphasized, however, on the usefulness of such models for the prediction of carbon free operating conditions. Reference [5] only compared the results obtained from a heterogeneous one-dimensional model with a two-dimensional one, while in a more recent study Pedernera et al. (2003) used their heterogeneous two-dimensional model for proposing some theoretical improvements which may influence the primary reformer performance in a good manner. [21] However, their model predicted a very large radial gradient, more than 100 °C, between the center of the tubes and the wall, which is in contrast with the results obtained for conventional steam reformers by others (Rostrup-Nielsen, 1984, De Deken et al., 1982, and NIPC, 2005). [25, 5, 7]

In the present study, the steady-state operation of a large-scale Midrex® reformer is investigated by means of a rigorous mathematical model, accounting for both furnace-side and reactor-side equations.

IV. FURNACE-SIDE MODELING

Among different types of radiative models appropriate for simulation of the fire-box section of an industrial steam reformer, a Roesler flux-type model reevaluated by Filla (1984) is applied for the furnace-side modeling. The governing equations in this model are as follow: [12]

$$\frac{\partial^2 F}{\partial z^2} = \alpha \left(\beta F + \gamma \right) \tag{9}$$

$$c_{p,fg} G_{fg} \frac{\partial T_{fg}}{\partial z} = 4 K_a \left(F - E_{fg} \right) + Q \tag{10}$$

In which:

$$\alpha = -(2K_a + A_t + A_r)/2 \tag{11}$$

$$\beta = -(4K_a + 2\varepsilon_t A_t) \tag{12}$$

$$\gamma = (4K_a E_{fg} + 2\varepsilon_t A_t E_t) \tag{13}$$

with boundary conditions:

$$\frac{dF}{dz} = 0 \qquad \text{, at } z = 0 \quad \& \quad z = L \tag{14}$$

$$T_{fg} = \sqrt[4]{F/\sigma} \qquad \text{, at } z = 0 \tag{15}$$

In the above equations Q is the heat released along the flame length due to combustion of fuel and air mixture. It can be readily found based upon the heat release pattern proposed by Roesler (1967). [24]

V. REACTOR-SIDE MODELING

All material and energy balance equations are written for a differential control volume of a single tube representing any other tube (Fig. 1). It is assumed that axial dispersion effects and external heat and mass transfer resistance are negligible; therefore, the mass balance equations for two major components, i.e. methane and carbon-dioxide under steady-state conditions are:

$$\frac{\partial x_{CH_4}}{\partial z} = \frac{D_{er} \rho_{pg}}{G} \left[\frac{1}{r} \frac{\partial x_{CH_4}}{\partial r} + \frac{\partial^2 x_{CH_4}}{\partial r^2} \right] + \frac{\rho_B r_i \eta_i M_{w,0}}{G y_{CH_4,0}} \tag{16}$$

$$\frac{\partial x_{CO_2}}{\partial z} = \frac{D_{er} \rho_{pg}}{G} \left[\frac{1}{r} \frac{\partial x_{CO_2}}{\partial r} + \frac{\partial^2 x_{CO_2}}{\partial r^2} \right] + \frac{\rho_B r_i \eta_i M_{w,0}}{G y_{CH_4,0}} \tag{17}$$

The energy balance equation can be written as:

$$G c_{p,pg} \frac{\partial T_{pg}}{\partial z} = \left[\lambda_{er} \left(\frac{1}{r} \frac{\partial T_{pg}}{\partial r} + \frac{\partial^2 T_{pg}}{\partial r^2} \right) + \rho_B \left(\sum_{i=1}^{2} (-\Delta H_i) r_i \eta_i \right) \right] \tag{18}$$

In which λ_{er} and D_{er} are effective radial conductivity and diffusivity respectively. They are generally calculated by heat and mass analogy:

$$Pe_{rm} = Pe_{rh} = Pe_{rf} \tag{19}$$

The methods for the calculation of fluid radial Peclet number, Pe_{rf}, will be discussed later.

Tallmadge (1970) proposed an extension of Urgan's (1952) equation apposite for estimation of pressure drop under higher Reynolds numbers: [28, 10]

$$-\frac{dp}{dz} = f \frac{\rho_{pg} u_{pg}^2}{d_{cat}} \tag{20}$$

$$f = \frac{1-\upsilon}{\upsilon^3} \left[m + \frac{n(1-\upsilon)}{\text{Re}} \right] \tag{21}$$

$$m = 1.75 \tag{22}$$
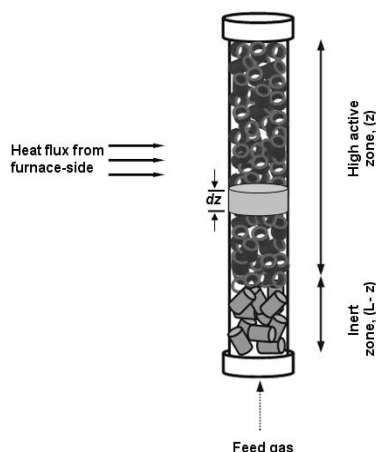
$$n = 4.2 \, \text{Re}^{5/6} \tag{23}$$

Fig. 1 Schematic of a reformer tube

VI. REACTION KINETICS AND RATE EXPRESSION

Any pair of reversible reforming reactions (Eq. (1) – (4)) will account for the stoichiometry of methane reforming. While the choice of equations is important when dealing with kinetic relationships, any pair of them may be selected when dealing with equilibrium relationships. In the present study, reactions (1) and (3) are considered.

The rates of these reactions are evaluated by the following first-order kinetic expressions:

$$r_1 = a_1 p \exp\left(\frac{-E_{a1}}{RT}\right)\left(y_{CH_4} - \frac{y_{H_2}^3 \cdot y_{CO} \cdot p^2}{y_{H_2O} \cdot K_{eq1}}\right) \quad (24)$$

$$r_3 = a_3 p \exp\left(\frac{-E_{a3}}{RT}\right)\left(y_{CO} - \frac{y_{H_2} \cdot y_{CO_2}}{y_{H_2O} \cdot K_{eq3}}\right) \quad (25)$$

The values of activation energy and the pre-exponential factor for the methane reforming reaction (Eq.24) are reported by Akers and Camp (1955), while the corresponding values for the water-gas shift reaction (Eq.25) are reported by Singh and Saraf (1979).[1, 27] The values of equilibrium constant (K_{eq}) for all reactions are reported by Elnashaie et al (1990). For first-order reversible reactions, the effectiveness factor can be calculated by the following expression (Froment and Bischoff, 1990): [9, 13]

$$\eta = \frac{1}{3\Theta^2}[(3\Theta)\coth(3\Theta) - 1] \quad (26)$$

In which the general Thiele modulus, Θ, is defined as:

$$\Theta = \frac{V_{cat}}{S_{cat}}\sqrt{\frac{k\rho_{cat}}{D_e} \cdot \frac{1 + K_{eq}}{K_{eq}}} \quad (27)$$

VII. BOUNDARY CONDITIONS

At reactor inlet:

$$x_{CO2} = x_{CH4} = 0 \quad (28)$$
$$T_{pg} = T_{feed} \quad (29)$$
$$P_{pg} = P_{feed} \quad (30)$$

At tube center:

$$\frac{\partial x_{CH_4}}{\partial r} = \frac{\partial x_{CO_2}}{\partial r} = 0 \quad (31)$$
$$\frac{\partial T}{\partial r} = 0 \quad (32)$$

At the tube inside walls:

$$\frac{\partial x_{CH_4}}{\partial r} = \frac{\partial x_{CO_2}}{\partial r} = 0 \quad (33)$$
$$\lambda_{er}\frac{\partial T_{pg}}{\partial r} = U_{in}(T_{t,out} - T_{pg}) \quad (34)$$

Where the overall heat transfer coefficient is defined as based on the inner surface tubes:

$$\frac{1}{U_{in}} = \left(\frac{d_{t,in}}{2k_t}\ln\frac{d_{t,out}}{d_{t,in}} + \frac{1}{h_{fw}}\right) \quad (35)$$

VIII. HEAT TRANSFER PARAMETERS

Special cares should be taken when certain heat transfer correlations are applied. The heat transfer resistance through the packing and fluid inside the bed is described by the effective radial thermal conductivity λ_{er}, which lumps together all heat transfer mechanisms. The extra resistance near the wall, causing the well known 'temperature jump', is described by an apparent wall heat-transfer coefficient (Logtenberg and Dixon, 1998).[19] The most important wall heat-transfer correlation ever used (Hyman, 1968, Singh and Saraf, 1979,

Ravi et Al., 1989, Murty and Murthy, 1988, and Rajesh et al. 2000) in simulating steam-reformers is the correlation of Beek (1962).[16, 27, 20, 23, 22, 2] In these studies, however, a correction factor of about 0.38-0.4 is applied to moderate the results predicted by this correlation. The reason may lie in the fact that the correlation of Beek (1962) is developed to predict the heat transfer near the wall of the tubes in which the temperature of the process gas is considerably higher than the mean cross-sectional temperature of fluid. [2]

A better and more rational solution is to define an overall heat transfer based on the two-dimensional heat transfer parameters as recommended by Froment (1990) as follows: [13]

$$\frac{1}{U_{in}} = \left(\frac{d_{t,in}}{2k_t}\ln\frac{d_{t,out}}{d_{t,in}} + \frac{1}{h_{fw}} + \frac{d_{t,in}}{CORR.\lambda_{er}}\right) \quad (36)$$

Beek (1962) stated that the value of *CORR* is equal to 8. According to Golebiowski (1973), Crider gives the value of 6.133.[14] Borkink and Westerterp (1992) fitted their experimental results by a *CORR* value of 7.4 for various types of packings.[13] A comprehensive review on the value of *CORR* has been carried out by Derkx and Dixon (1996).[6] It appears that this remains an issue which has yet to be completely solved. In the present study, the value of *CORR* is assumed to be 6.133. The most commonly used equations for the heat-transfer coefficient at the wall are compiled in Table I.

The correlations found in the literature for the effective radial thermal conductivity, λ_{er}, are semi-empirical expressions derived from various experimental results (Kvamsdal et al., 1999). Generally, the value of effective radial thermal conductivity is chosen from an effective radial Peclet number. The latter is defined as (Gunn, 1987):[17, 15]

$$\frac{1}{Pe_{rf}} = \frac{1}{Pe_{rf(\infty)}} + f((Re.Pr)^{-1}) \quad (37)$$

TABLE I
CORRELATIONS FOR HEAT-TRANSFER COEFFICIENT AT WALL (N = dti /dcat)

	Wall to Fluid Heat Transfer Correlations	Ref.
Beek	$Nu_{fw} = 2.58(Re.Pr)^{1/3} + 0.094(Re)^{0.8}(Pr)^{0.4}$	[14]
Yagi & Kuni	$Nu_{fw} = \dfrac{0.054\,(Re\,.Pr)}{1 + 0.0135\,(Re)^{0.5}(Pr)^{0.66}}$	[14]
Leva	$Nu = 0.813\exp(-6/N)\,(Re)^{0.9}$	[14]
Dixon & LaBua	$Nu_{fw} = (1 - 1/N)(Re)^{0.610}(Pr)^{1/3}$	[30]
Li & Finlayson	$Nu_{wf} = 0.17(Re)^{0.79}(Pr/0.72)^{1/3}$	[18]

This equation shows that Peclet number for heat-transfer becomes independent of the Reynolds number at high values (Re>1000), governing the operation of all conventional steam reformers. Different values/correlations proposed for prediction of limiting value for Peclet number ($Pe_{rf(\infty)}$) are presented in Table II. Steam reforming standard catalysts are ring-shaped types; therefore, another important issue that should be considered in applying heat transfer equations is the packing shape used in deriving those equations. In the present study, the values reported by Borkink and Westerterp (1992)

are applied, while, the equivalent diameters of catalysts are calculated as: [3]

$$d_{cat} = \sqrt[3]{6V_{cat}/\pi} \quad , \text{ for heat transfer} \tag{38}$$

$$d_{cat} = 6V_{cat}/S_{cat} \quad , \text{ for pressure drop} \tag{39}$$

TABLE II. CORRELATIONS/VALUES RECOMMENDED LIMITING PECLET NUMBER FOR HEAT TRANSFER, ($N = dti /dcat$)

Correlations for Prediction of Fluid radial Peclet number for Heat Transfer		Ref.
Fahien and Smith	$Pe_{rf(\infty)} = A(1 + 19.4/N^2)$	[3]
	Typical values for A: A = 10 for spheres A = 5 for nonspheres	
Schlunder	$Pe_{rf(\infty)} = A(2 - (1 - 2/N)^2)$	[3]
	Typical values for A: A = 7 for spheres A = 4.6 for nonspheres	
Borkink and Westerterp	$Pe_{rf(\infty)} = 10.9$ for spheres $Pe_{rf(\infty)} = 7.6$ for cylinders $Pe_{rf(\infty)} = 4.2$ for rings	[3]
Dixon	$Pe_{rf(\infty)} = 12$ for spheres $Pe_{rf(\infty)} = 7$ for cylinders $Pe_{rf(\infty)} = 6$ for rings	[29]

IX. SOLUTION PROCEDURE

The solution starts with an initial guess for the tube-skin outer surface temperature. By means of this value, the furnace-side and reactor-side equations are solved separately. The new value for the tube-skin temperature can be calculated by making an energy balance on the tubes:

$$U_{out}(T_{t,out} - T_{pg}) = \varepsilon_t (F - E_t) \tag{40}$$

Convergence is assumed to have been achieved whenever the maximum difference between two sequential steps is less than the convergence criterion. All hydrocarbons heavier than methane in the feed are assumed to instantaneously hydrocrack into CH_4 and CO. The thermodynamic properties of combustion products and process gas are obtained by using *S.R.K* equation of state, while their transport properties are obtained from *DIPPR* reported data (Daubert and Danner, 1991). [4]

X. MODEL VALIDATION

In order to validate the model, the simulation results from both one-dimensional and two-dimensional modeling are compared against the available data of a Midrex® direct reduction plant. The furnace and process conditions of this unit are listed in Tables III and IV.

TABLE III PLANT FURNACE DATA

Furnace dimension (L × W × H), (m)	41 × 15 × 8
total number of tubes	432
reformer tubes inside diameter , (m)	0.200
reformer tubes outside diameter , (m)	0.224
heated length of reformer tubes , (m)	7.9
total number of burners	168
emissivity of tubes	0.85
flame length ,(m)	4

TABLE IV
MOBARAKEH PLANT OPERATING CONDITIONS

Fuel flow rate, (Nm^3/hr)	45198
Combustion air flow rate, (Nm^3/hr)	126390
Fuel inlet temperature, (K)	310
Combustion air Inlet temperature, (K)	873
Fuel & air mixture inlet temperature, (K)	697
Feed gas flow rate, (Nm^3/hr)	107122
Feed inlet temperature, (K)	673
Inlet pressure of feed gas, (kPa)	246

mole %	CH_4	C_2H_6	C_3H_8	C_4H_{10}	H_2	H_2O	CO	CO_2	N_2
Feed	14.99	1.4	0.53	0.19	35.02	13.64	18.95	14.24	1.03
Fuel	6.79	0.44	0.16	0.06	43.95	6.11	23.77	17.76	0.99

XI. RESULTS AND DISCUSSIONS

A. Output Conditions

The reactor and furnace output conditions predicted by different one and two-dimensional models are gathered in Tables V-VII.

TABLE V
FURNACE AND TUBE OUTPUT RESULTS PREDICTED BY DIFFERENT TWO-DIMENSIONAL MODELS (SPHERE PELLETS)

Heat Transfer Correlation based on Sphere Pellets	Flue Gas Temperature, (K)	Process Gas Temperature, (K)	Effluent Methane Mole Fraction, (%)
Beek	1323	1159	1.82
Yagi & Kuni	1365	1158	2.22
Leva	1358	1161	2.19
Dixon & LaBua	1323	1189	1.69
Li & Finlayson	1325	1180	1.84
Plant Data	1393	1198	1.90

An overview of the results reveals that in most cases one dimensional model can predict the reactor output conditions very well. However, reasonable predictions by two-dimensional models can only be achieved when certain correlations for wall to fluid heat transfer and the radial Peclet number are applied. As predicted before, the shape of catalyst and the type of heat transfer correlations have considerable effects on final results. The best results for both furnace and reactor outputs are predicted when the correlation of Yagi is used accompanied by a proper value of the limiting radial Peclet number for ring-shaped catalysts. On the other hand, if the catalysts are assumed to be spherical, the best results are obtained by using the correlation of Beek, followed by the correlation of Li & Finlayson (1977) (Table 1).[18] In all cases, one-dimensional models have a better estimation for flue gas temperature.

TABLE VI
FURNACE AND TUBE OUTPUT RESULTS PREDICTED BY DIFFERENT TWO-DIMENSIONAL MODELS (RING PELLETS)

Heat Transfer Correlation based on Ring Pellets	Flue Gas Temperature, (K)	Process Gas Temperature, (K)	Effluent Methane Mole Fraction, (%)
Beek	1312	1218	1.41
Yagi & Kuni	1346	1185	1.88
Leva	1334	1193	1.78
Dixon & LaBua	1302	1222	1.32
Li & Finlayson	1313	1216	1.42
Plant Data	1393	1198	1.90

TABLE VII
F FURNACE AND TUBE OUTPUT RESULTS PREDICTED BY
DIFFERENT TWO-DIMENSIONAL MODELS (RING AND SPHERE
PELLETS)

Heat Transfer Correlation based on Ring and Sphere Pellets	Flue Gas Temperature, (K)	Process Gas Temperature, (K)	Effluent Methane Mole Fraction, (%)
Beek	1353	1198	1.81
Yagi & Kuni	1353	1198	1.80
Leva	1346	1203	1.74
Dixon & LaBua	1342	1205	1.67
Li & Finlayson	1354	1097	1.81
Plant Data	1393	1198	1.90

B. Process Gas Temperature Profiles

Axial and radial temperature profiles are shown by a three dimensional graphs in Fig. 2 for the correlation of Yagi. Since the best results are obtained by the correlation of Beek for spherical catalyst and by the correlation of Yagi for ring-shaped catalyst, the temperature gradient profiles between the wall and center of tubes are also drawn in Figure 3 for these two models.
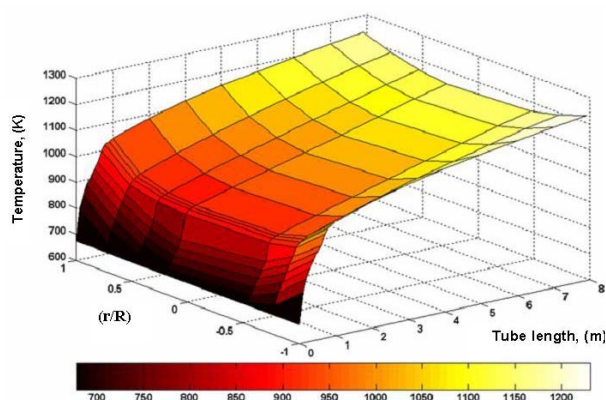

Fig. 2 Radial and axial temperature profile inside the

As expected, the radial temperature gradients in Midrex[®] reformer tubes are considerably higher than those in conventional steam reformers due to the lower process Reynolds numbers, higher ratio of tube diameter to tube length, and lower feed gas temperature. While the maximum temperature gradient between the bed centerline and the wall is predicted to be 190 ^{o}C for sphere catalysts, the corresponding value is 130 ^{o}C for ring-shaped catalysts. To have an apposite measure, the developed model was applied to simulate a conventional steam reformer used in a MeOH plant (NIPC, 2005).[7] The average superficial process Reynolds number for this plant is about 6000, up to 2.5 times that of a Midrex[®] reformer. The results show that the maximum temperature difference in this reformer is 49 ^{o}C. This is in agreement with the value of 33 ^{o}C reported by De Deken et al (1982) for another conventional steam reformer used in an Ammonia plant. It should be reminded that the average superficial process Reynolds number for an Ammonia plant steam reformer is typically higher than that of a MeOH plant steam reformer. A better view on Fig. 3 shows that when the catalysts are assumed to have spherical shapes, more temperature gradients exist between the tube center and the tube wall.[5]
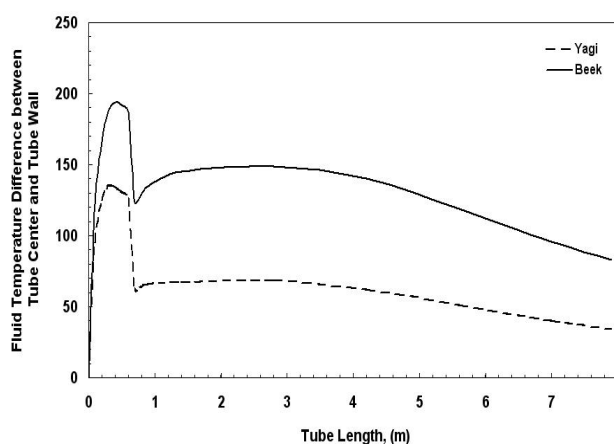

Fig. 3 Effect of heat transfer model on fluid temperature difference between tube center and tube wall

The reason for this can be clarified by looking at Table 2, in which it is clear that ring-shaped catalysts have higher effective radial conductivity resulting in a lower radial temperature difference inside the tubes. In both cases, it can be seen that the radial temperature gradients will be considerably decreased in the active catalyst zone in comparison with the inert zone. In fact, after contacting with the active catalyst, the process gas loses its temperature due to the occurrence of highly endothermic reforming reactions. Since the furnace heat load reaches the catalyst bed via tube walls, the temperature of process gas is first increased near the walls and then is conducted to the tube center in a radial direction. Consequently, the process gas temperature is constantly higher close to the wall than close to the center of the tubes; therefore, the rate of reforming reactions is more rapid near the wall. As a result, the radial temperature difference between the wall and the center of the reformer tubes will be lower in the active catalyst zone than in the inert catalyst zone. Another noticeable feature which can be observed from these figures is the continued existence of the process gas temperature gradient throughout the total length of tubes. The radial temperature differences between the tube centerline and the wall reach 35 ^{o}C and 80 ^{o}C for spherical and ring-shaped catalysts, respectively.

C. The Effect of Catalyst Loading Profile

The radial and axial methane fractional conversion profile is shown in Fig. 4. As stated above, the reformer feed gas is far above the equilibrium condition, resulting in an undesirable situation in which the reforming reactions will not proceed unless the feed gas temperature rises before contact with the nickel catalyst zone. In real operational conditions, catalyst loading involves the utilization of non-active materials at the bottom of the catalyst bed. This will provide an inert zone in which the temperature of process gas will be increased above the upper limit of carbon formation reactions, and the lower limits of reforming reactions.
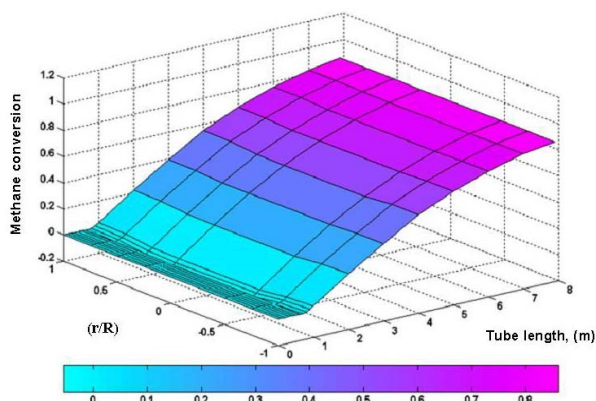
Fig. 4 Methane radial and axial fractional conversion inside the reformer tube

The effect of this catalyst loading profile on the thermal and process performance of the reformer can be better understood from Figures 3 and 5 in which a conversion drop is apparent at the interface between different catalyst zones, especially in the center of the tubes, due to the considerable temperature gradients between the wall and the center of the tubes. The process gas temperature drops between the catalyst bed centerline and the wall at the interface is about 60 $^{\circ}$C for both models using the correlations of Yagi, and the correlations of Beek. However, no temperature drop is seen along the tube length in the axial direction. As is shown in Fig. 5, the conversion of methane is negative in the first segments of the active catalyst zone, meaning that the reversed reactions happened. The calculation results show that the temperature rise in the inert zone is approximately five times greater than in the active zone. As a result, when the hot feed gas reaches the high active catalyst, the endothermic reforming reactions will occur very rapidly and will cool the feed gas back down into an undesirable zone for forward reforming reactions, especially in the center of tubes where the risk of carbon deposition is also high. It comes into question whether the length of the inert catalyst zone should be increased or not?
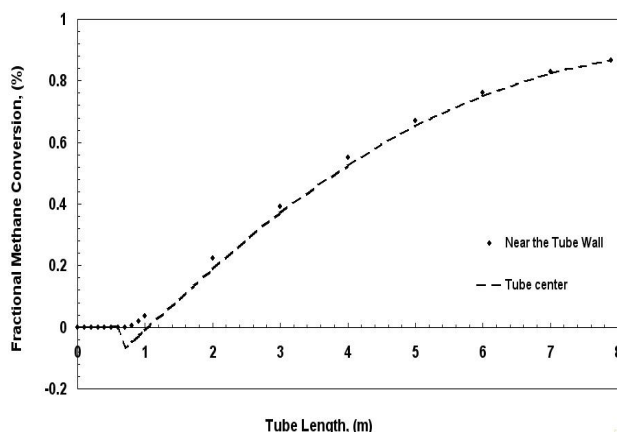
If this length is increased, the feed will have a greater temperature when it comes into contact with the active zone, and the rate of reforming reactions will be more rapid; as a result, a higher temperature drop on the active zone will happen again. This, in turn, will enhance the risk of reversed reforming reactions as well as carbon formation. Therefore, the safe design may not be achieved. On the other hand, if the amount of inert catalyst is lowered, the temperature of the feed may not reach the proper temperature required for reforming reactions, and the risk of carbon deposition will be enhanced again. A conclusive solution needs more comprehensive investigations including the optimization of process conditions and the use of dual or triple catalyst loading profiles inside the reformer tubes (Sadri et al., 2007). [26]

D. Tube wall Temperature

Tube wall temperature is an important parameter in design and operation of steam reformers. The tube material is exposed to an extreme thermal environment. Higher temperatures at the tube wall, and thus within the tube, lead to increased carbon lay-down on the catalyst and a consequential loss of catalytic activity as well as potential catalyst breakage resulting in increased pressure drop and hence, low flow. Both lead to a decrease in the local reaction rate and associated endotherm. A common rule of thumb is that a tube wall temperature increase of 20 °C will foreshorten a tube life by over 50 % from its design period of 10 years to less than 5 years [8]. An apparent mistake seen in published works is the assumption at which the outside tube skin temperature is considered to be identical for both one and two dimensional models [5, 21]. This is clearly a false assumption, because there is a substantial temperature difference between the average fluid temperature in one dimensional models and the fluid temperature flowing near the inner wall of tubes in two dimensional models, particularly in the first half length of reformer tubes. As a result, the temperature gradient between the furnace gas and process gas and consequently the tube wall temperature, will differ in these models. The tube temperature profiles obtained from one and two dimensional models are shown in Fig. 6.

Fig. 5 Methane conversion in center and next to the wall of a reformer tube (two-dimensional model)
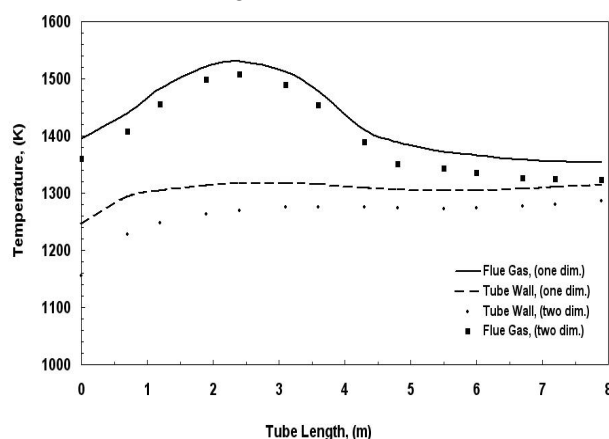

Fig. 6 The difference between the results obtained by one and two dimensional models on tube wall temperature

From this figure, it is seen that the one-dimensional model apparently predicts higher values for tube wall temperatures. The flue gas temperature profiles inside the furnace are also shown in this figure showing that this variable has higher values in the one-dimensional model too. Therefore, it can be inferred that the one dimensional model performs the total heat balance total of a steam reformer box (furnace and tubes) at a higher level than does the two-dimensional model.

XII. CONCLUSION

The giant quantity of heat transfer models proposed in open literatures for studying fixed bed catalytic reactors during the last 40 years, comes most likely from a lack of understanding of how exactly heat transfer in a fixed bed catalytic reactor should be described and modeled. Due to the considerably lower operating Reynolds number, lower tube length to diameter ratio, together with the non-availability of extra steam in the feed gas, causing a large temperature gradients in radial dimension, the operation of steam reformers used for production of reducing gas may be a suitable case to examine the accuracy of theoretical heat and mass transfer correlations proposed in open literatures for studying the behavior of packed-bed catalytic reactors under real conditions. For that reason, a rigorous two-dimensional model is developed for simulating the operation of this less investigated-type steam reformer. Both the process side and furnace side have been included in this integrated model. The model is capable of not only predicting reactor output conditions based on longitudinal changes, but also inspecting radial heat and mass transfer inside the tubes. A number of heat transfer models predicting values for effective radial conductivity and diffusivity have been examined during the simulation of reactor side. Simulation results have been tested against available data from an actual plant. A comparison between the calculated and available data shows that the two dimensional models can represent the reactor and furnace actual data very well but not exceptional. In all cases, strong radial temperature gradients inside the reformer tubes have been found. In some cases, the results show substantial discrepancy between these models, and it is revealed that reasonable predictions in all aspects, such as effluent composition and tube-wall maximum temperature, can only be achieved when certain correlations for wall to fluid heat transfer equations are applied. The two dimensional heat transfer model in the catalyst bed may seem to be more accurate than the one-dimensional model at first glance. However, in equations based on the former model, the linear dimension of the catalyst likewise does not adequately denote the effect of the form and size of the catalyst on heat transfer [14]. The changes of the effective thermal conductivity of the bed along the radius due to non-uniform flow, effects of chemical reaction over the catalyst, and the system of catalyst packing also not considered in deriving most of these equations. Moreover, it should be noted that the two dimensional model is not completely adequate for describing a packed bed in which the value of $N (= d_{ti}/d_{cat})$ exceeds 10 [14]. Because of high accuracy, one-dimensional models are yet comparable with two-dimensional ones in many aspects; however, developing two-dimensional models are necessary when the effect of catalyst loading profile and risk of carbon formation are the matters of concern in designing steam reformers.

NOMENCLATURE

a_i pre-exponential factor for reaction i, i=1, 3, (kmol/kg$_{cat}$. s)

A_t half tube surface area per unit free volume, (m^2/m^3)

A_r half of refractory surface area per unit free volume, (m^2/m^3)

c_p specific heat at constant pressure, (J/kg. K)

d diameter, (m)

D_e effective diffusivity of gas components, (m^2.s)

D_{er} effective radial diffusivity, (m^2.s)

E black body emissive power, (W. m^2)

E_a energy of activation, (J. mol)

f parameter defined by Eq.21

F half-sum of forward and backward axial fluxes, (kW. m^2)

G mass velocity, (kg/m^2 s)

h_{fw} fluid-wall heat-transfer coefficient, (W/m^2 .K)

ΔH heat of reaction, (J/mole)

k reaction rate constant, (kmol/ kg$_{cat}$. S. Pa)

k_t thermal conductivity of tube material, (W/m^2 .K)

K_a furnace gas absorption coefficient, (1/m)

K_{eq} equilibrium constant

L tube length, (m)

m parameter defined by Eq.22

M_w molecular weight, kg kmol^{-1}

n parameter defined by Eq.23

p pressure, (Pa)

Pe_{rf} fluid radial Peclet number, dimensionless

$Pe_{rf(\infty)}$ limiting value for Peclet number, dimensionless

Pe_{rh} effective radial Peclet number for heat, dimensionless

Pe_{rm} effective radial Peclet number for mass, dimensionless

Pr   Prandtl number, dimensionless

Q fuel calorific value, (W/ m^2)

r radial distance, (m)

r_i rate of reaction i, i=1, 3, (kmol/kgcat. S)

R universal gas constant, 8.314 (J/mol. K)

Re   Reynolds number based on superficial mass velocity, dimensionless

S   surface, (m^2)

T temperature, (K)

U overall heat transfer coefficient, (W/m^2. K)

V   volume, (m^3)

x conversion of reactants, dimensionless

y mole fraction of gas components, dimensionless

z axial distance, (m)

Greek Symbols

α parameter defined by Eq.11

β parameter defined by Eq.12

γ parameter defined by Eq.13

ρ density, (kg/m^3)

Θ Thiele modulus defined by Eq.27

σ Stefan-Boltzmann constant, 5.667e^{-8} (W/m^2. K^4)

υ	catalyst bed void fraction, dimensionless
ε	emissivity
λ_{er}	effective radial thermal conductivity, (kW. m^2. K)
η_i	effectiveness factor i, i=1, 3, dimensionless

Subscripts

B	catalyst bed
cat	catalyst
fg	flue gas
in	inner surface of tubes
0	initial condition
out	outer surface of tubes
pg	process gas
r	refractory
t	tube
fw	fluid to wall
ti	tube internal diameter

REFERENCES

[1] Akers, W. W., Camp, D.P., "Kinetics of the Methane-Steam Reaction", *AIChE. J.* 4 (1955) 471-474.
[2] Beek, J., "Advances in Chemical Engineering", Vol. 3, Academic Press, New York (1962).
[3] Borkink, J. G. H., Westerterp, K. R., "Influence of Tube and Particle Diameter on Heat Transfer in Packed Beds", *AIChE. J.* 38 (1992) 703-715.
[4] Daubert, T.E., Danner, R.P., Design Institute for Physical Property Data, American Institute of Chemical Engineers, Hemispher Publishing (1991).
[5] De Deken, J. C., Devos, E. F., Froment, G. F., "Steam Reforming of Natural Gas: Intrinsic Kinetics, Diffusional Influences, and Reactor Design", *Chemical Reaction Engineering, ACS Symp. Ser.,* 196, Boston (1982).
[6] Derkx, O. R., Dixon, A. G.," Determination of the Fixed Bed Wall Heat Transfer Coefficient using Computational Fluid Dynamics", *Numer. Heat Transfer*, Part A, 29 (1996) 777-785.
[7] Design and Construction of a Methanol Pilot Plant Based on Reforming Technology, National Iranian Petrochemical Company (NIPC) Project NO. 81118018, Iran (2005).
[8] Dixon, A.G., Nijemeisland, M., Stitt., E.H, "CFD Study of Heat Transfer near and at the Wall of a Fixed Bed Reactor Tube: Effect of Wall Conduction", *Ind. Eng. Chem. Res.* 44 (2005).
[9] Elnashaie, S. S. E. H., Soliman, M.A., Al-Ubaid, A.S., Adris, A., "On the Non-monotonic Behavior of Methane-Steam Reforming Kinetics", *Chem. Eng. Sci.,* 45 (1990) 491-501.
[10] Ergun, S., "Fluid Flow through Packed Beds" *Chem. Eng. Prog.* 48 (1952) 89-94.
[11] Farhadi, F., Motamed Hashemi, M.M.Y., Bahrami Babaheidari, M., "Modeling and Simulation of Syngas Unit in Large Scale Direct Reduction Plant", *Ironmaking and Steelmaking*, 30 (2003) 35-41.
[12] Filla, M., "An Improved Roesler-type Flux Method for Radiative Heat Transfer in One-dimensional Furnaces", *Chem. Eng. Sci.* 39 (1984) 159-161.
[13] Froment, G. F., Bischoff, K. B., Chemical Reactor Analysis and Design, Wiley, New York (1990).
[14] Golebiowski, A., Wasala, T., "Thermal Processes in Catalytic Reforming of Methane with Water Vapor", *International Chem. Eng.*, 13 (1973) 133-139.
[15] Gunn, D. J., "Axial and Radial Dispersion in Fixed Beds", *Chem. Eng. Sci.* 42 (1987) 363-373.
[16] Hyman, M.H., "Simulate Methane Reformer Reactions", *Hydrocarbon. Process.* , 49 (1968) 131-137.
[17] Kvamsdal, H. M., Svendsen, H. F., Olsvik, O., "Dynamic simulation and Optimization of a Catalytic Steam Reformer", *Chem. Eng. Sci.* 54 (1999) 2697-2706.
[18] Li, C., Finlayson, A., "Heat Transfer in Packed Beds-A Reevaluation", Chem. Eng. Sci. 32 (1977) 1055-1066.
[19] Logtenberg, S. A., Dixon, A. G., "Computational Fluid Dynamics Studies of the Effects of Temperature-Dependent Physical Properties on Fixed-Bed Heat Transfer", *Ind. Eng. Chem. Res*., 37 (1998) 739-747.
[20] Murty, V.S., Murthy, M.V.K., "Modeling and simulation of a top-fired reformer",*Ind. Eng. Chem. Res* 27 (1988) 1832-1840.
[21] Pedenera, M. N., Pina, J., Borio, D.O., Bucala, V., "Use of a Heterogeneous Two-dimensional Model to Improve the Primary Steam Reformer Performance", *Chem. Eng. J.* 94 (2003) 29-40.
[22] Rajesh, J.K., Gupta, S.K., Ray, A.K., "Multiobjective optimization of steam reformer performance using genetic algorithm", *Ind. Eng. Chem. Res*. 39 (2000) 706-717.
[23] Ravi, K., Joshi, Y. K., Guha, B. K., "Simulation of Primary and Secondary Reformers for Improved Energy Performance of an Ammonia Plant", *Chem. Eng. Technol*. 12 (1989) 358-364.
[24] Roesler, F.C., "Theory of radiative heat transfer in co-current tube furnaces", *Chem. Eng. Sci.* 22 (1967) 1325-1336.
[25] Rostrup-Nielsen, J. R., *Catalysis. Sci. Technology*, Vol IV, Springer, Berlin (1984).
[26] Sadri, M., Vakhshouri, K., Motamed Hashemi, M. M. Y, "Coke Formation Possibility during the Production of Reducing Gas in Large Scale Direct Reduction Plant", *Ironmaking and Steelmaking*, 34 (2007) .
[27] Singh, C. P. P., Saraf, D. N., "Simulation of side-fired hydrocarbon reformers", *Ind. Eng. Chem. Process. Des. Dev* 18 (1979) 1-7.
[28] Tallmadge, J. A., "Packed Bed Pressure Drop-An Extension to Higher Reynolds Numbers", *AIChE. J.* 19 (1970) 1092-1093.
[29] Dixon, A. G., "Wall and Particle –Shape Effects on Heat Transfer In Packed Beds Transfer in Fixed Beds at Very Low Tube-to-Particle Diameter Ratio", *Chem. Eng. Communication,* 71 (1988) 217-237.
[30] Dixon, A. G., "Heat Transfer in Fixed Beds at Very Low Tube-to-Particle Diameter Ratio", *Ind. Eng. Chem. Res*. 36 (1997) 3053-3064.